Framework Programme 7, PEOPLE programme, Marie Curie Initial Training Networks (ITN)

GMES Initial Operations – Network for Earth Observation Research Training

European Centre of Excellence in Earth Observation Research Training

Project Coordinator:
Professor Heiko Balzter
University of Leicester, UK
email: hb91@le.ac.uk

Deliverable D1

"Deforestation map of the Congo basin from 1996 to the present"

Work Package 2.1

28 February 2014

Authors: Wheeler, J., Tansey, K., Balzter, H. and Nicolas-Perea, V.

GIONET was funded by the European Commission, Marie Curie Programme, Initial Training Networks, Grant Agreement number PITN-GA-2010-264509.

TABLE OF CONTENTS

1 Executive summary 3
2 Introduction 3
2.1 Contribution of Remote Sensing 5
2.2 Aims and Objectives 9
3 Methodology 9
3.1 Study Area 9
3.2 Data 12
3.3 Processing steps for objective 1: optical and SAR forest cover classification comparison 15
3.4 Processing steps for objective 2: Supervised classifications of improved K&C Initiative ALOS-PALSAR mosaics 17
4 Results 19
4.1 Objective 1: optical and SAR forest cover classification comparison 19
4.2 Objective 2: Supervised classification of improved K&C Initiative ALOS-PALSAR mosaics 20
5 Conclusions 26
5.1 Future work 27
6 References 28

1 EXECUTIVE SUMMARY

This study investigates the use of wide area L-band Synthetic Aperture Radar (SAR) mosaics to derive an improved forest/non-forest (FNF) map at 50m resolution of the Congo Basin. The study is described in two sections: the first, a comparison of single year wide area optical- and SAR-derived FNF maps to establish their respective strengths and limitations; the second, a comparative analysis of several SAR classification techniques of a smaller five degree square region over a period of 3 years (2007-2010) to develop a proof of concept for a future implementation of the optimal technique over the entire Congo Basin. The principal dataset was the Japanese Space Exploration Agency's (JAXA) Kyoto and Carbon Initiative mosaic from the Phased Array L-band Synthetic Aperture Radar (PALSAR) sensor on the Advanced Land Observing Satellite (ALOS). Several classification methods were used and the results compared with recently published optical and SAR-based FNF maps. For the Congo basin region studied, an average improvement in overall accuracy of 1.6% was shown over the previously published SAR-based FNF maps, as well as a visually clear increase in consistency in several areas of moisture related signal disturbance seen in the previous maps.

2 INTRODUCTION

Deforestation and forest degradation are a major source of natural and anthropogenic greenhouse gas emissions (Malhi & Grace, 2000). Stored carbon is released into the atmosphere when forests are felled, mostly from logging or burning to create land available for agriculture (FAO, 2010). Exposed and especially drained soil also releases carbon, which for certain soil types such as peat has been stored in greater volumes (as soil organic carbon, SOC) than in the living woody material (as above ground biomass, AGB) (Englhart *et al.* 2012). Conversion of forest to other land cover and land use types reduces the area available to store carbon and therefore reduces the ability to offset the increases of atmospheric carbon from fossil fuel emissions.

Deforestation in the context of this study refers to forest loss, where the land cover type has changed from forested land to non-forested land (UNFCCC, 2001). Forest degradation refers to loss of forest where the land cover type remains as forest but there is a reduction in the quality or density of tree cover. Deforestation and forest degradation are considered to be a major contributing factor towards climate change (Stocker *et al.*, 2013), particularly in the tropics (Bala *et al.*, 2007). Deforestation and forest degradation result in loss of biodiversity, and are specifically mentioned in the Convention for Biological Diversity's (CBD) 'Aichi Biodiversity Targets' as part of their 2011-2020 plan (CBD, 2010).

A key intergovernmental programme that has been created in recognition of the important role of tropical forests in climate change, and the potential benefits of their conservation, is the UN REDD programme (Reducing Emissions from Deforestation and forest Degradation in developing countries), which aims to incentivise reducing carbon emissions from forest loss in developing countries through financial means. The concept of REDD was introduced at the 11th Conference of Parties (COP-11) of the UN Framework Convention on Climate Change (UNFCCC) in 2005 (Herold & Johns, 2007), and after discussion and agreement in COP-13 in 2007, was officially launched in 2008. REDD now supports REDD+, which adds "conservation of forest stocks, sustainable management of forests, and enhancement of forest carbon stocks" to the climate change mitigating actions of REDD (UNFCCC, 2010). In order to achieve the goals of REDD, it is necessary to assess stocks of carbon contained in AGB in participating countries. AGB is measurable through a variety of direct and indirect methods, and fluctuations in AGB are the primary focus of monitoring, reporting and verification (MRV) systems necessary for REDD projects. Ultimately, participating nations should have in place an MRV system that can provide regular and consistent information about carbon stocks at a local and national level.

The Congo Basin contains the second largest continuous area of tropical forest in the world, yet is one of the least studied areas (Baccini *et al.* 2011). For reasons such as political instability, including numerous civil wars, and resulting lack of infrastructure, forest loss is not as severe in Africa compared with the two other major tropical forested continents, South America and Asia (Justice *et al.* 2001; Mayaux & Achard, 2010). For the same reasons, it has

been difficult to obtain reliable ground data, especially from the Democratic Republic of Congo, which contains roughly 60% of the Congo Basin's tropical forest area.

2.1 CONTRIBUTION OF REMOTE SENSING

Ground based forest inventories and remote sensing surveys from airborne and spaceborne platforms have merits and drawbacks in their suitability. Forest inventories provide the most direct and accurate method of assessing AGB of a particular plot, and are necessary for interpreting remote sensing data and validating results, but alone they are not practical for regular wide area surveys. A wholly ground-based approach involves sampling of a number of plots followed by data interpolation to cover gaps between sample plots and extrapolation of known average AGB in certain forest types to a wider area. Remote sensing has the potential for more consistent 'wall-to-wall', regular surveys of AGB, but there are multiple potential sources of error. Certain types of active sensors, to varying degrees of accuracy, can be used to directly or indirectly (through canopy height models and other established allometric relationships) measure AGB; principally height related metrics from an active optical system using laser pulses called LiDAR (Light Detection and Ranging) , and Synthetic Aperture Radar (SAR). A reliable wall-to-wall forest/non-forest map can be used to improve methods of AGB modelling by facilitating interpolation between known or modelled values of AGB where there is spacing between samples (e.g. Saatchi *et al.* 2011).

LiDAR offers many opportunities for small and medium area retrieval of forest parameters, including forest height and structure, from high density pulsed laser signals. While there are projects underway in some tropical countries to achieve a country-wide baseline survey using airborne LiDAR (e.g. Gabon - White 2012) it is unfeasible at present for surveying the entire Congo basin. Spaceborne LiDAR, in the form of the Ice, Cloud and land Elevation Satellite's Geoscience Laser Altimeter System (IceSAT-GLAS) instrument, has been used to measure forest height characteristics, and from that AGB (Saatchi *et al.*, 2011), but this requires several additional datasets, including forest cover products and allometric data (species and coarser scale data that relate forest parameters such as average tree height, diameter at breast height, and AGB) for many forest areas. In addition, IceSAT-GLAS has been the only spaceborne

profiling LiDAR to date, and will not be replaced until IceSAT-2, scheduled for launch in 2016 (NASA, 2012).

Optical remote sensing techniques to measure deforestation exploit differences in reflectance of visible and near-infrared light between different ground targets. In this way, landcover types with different vegetation species and densities can be classified. Optical remote sensing is limited in tropical regions due to atmospheric interference and cloud cover, which can obscure all or part of the image. This can preclude the use of high spatial resolution imagery, which is restrained by narrower swaths and an infrequent acquisition cycle. For wide scale (i.e. global or continental) forest monitoring, several studies have employed a technique of wall to wall coverage using data from coarse spatial resolution (>100m pixel resolution) sensors such as ENVISAT-MERIS, TERRA-MODIS and NOAA-AVHRR, combined with sampled data from moderate spatial resolution (10-100m pixel resolution) sensors such as Landsat or SPOT (Hansen *et al.*, 2008; Hansen *et al.*, 2010; Potapov *et al.*, 2012). Since the coarse spatial resolution can provide global data coverage every one or two days, there is a much higher chance of acquiring cloud free imagery. However, processes of deforestation may occur at a scale finer than their pixel resolution, requiring the use of higher resolution data.

SAR is a side-looking active remote sensing system which transmits microwaves and receives measurements from the signal backscattered from a surface, to produce an image after appropriate processing. The longer wavelengths of microwaves allow imaging of the ground through cloud cover, and as it is an active system, images can also be gathered at night. In brief, imaging radar systems operate by emitting a pulsed beam to the side of the platform, and measuring the intensity (size of backscatter) and time taken for the signal to return. Signals that take longer to return are further from the sensor in the range direction (to the side, perpendicular to the direction of flight), and as the platform moves forward each pulse gives information about surface objects in the azimuth direction (along its track, or flight path). The frequencies of SAR range from around 0.3GHz up to 12.5 GHz for bands P to X, as seen in Table 1 (Rosenqvist *et al.*, 2007). Lower frequency SARs (i.e. L- and P- band), with longer wavelengths, have a greater ability to penetrate the surface and canopy cover. The signal interacts with objects at the same scale or larger than its wavelength, with smaller

objects not affecting the backscatter. As a result, longer wavelength SAR sensors are more suitable for forestry applications, in particular to measure AGB.

Table 1: Historical, current, and future spaceborne SAR satellites/sensors, with their wavelength and frequency ranges, adapted from (Rosenqvist et al. 2007)

Wavelength (cm)	**2.4**	**3.75**	**7.5**	**15**	**30**	**100**
Radar Band		**X**	**C**	**S**	**L**	**P**
Completed, **currently active**, *planned future* and *proposed future** SAR spaceborne sensors	1990-2000		ERS-1/2,	Almaz	JERS-1	
	2000-2010	**TerraSAR-X, Cosmo Skymed**	ENVISAT-ASAR, SRTM, **Radarsat-1/2,**		ALOS-PALSAR	
	2010-2020	**TanDEM-X**,	**Sentinel 1 A**/*B, Radarsat Constella-tion*	*NovaSAR-S*	*SAOCOM-1A/1B, ALOS-2, TanDEM-L**	*BIOMASS*
Frequency (GHz)	**12.5**	**8**	**4**	**2**	**1**	**0.3**

Emitted SAR signals are polarised in either horizontal (H) or vertical (V) planes, and the returned signal is similarly filtered in either horizontal or vertical planes. For example, an HV polarised SAR image has been emitted in horizontal polarisation and the vertically polarised component of the returned signal has been recorded. Due to polarisation-dependent differences in backscatter, the choice of polarisation depends on the desired application.

Several spaceborne SAR sensors have been used in the past 20 years to generate wide area mosaics in Central Africa. These involve the systematic gathering of hundreds of SAR data strips (extended along-track acquisitions). Major mosaics have been generated in C- and L-band (bands between the frequency ranges of 4 – 8 GHz and 1 – 2 GHz, respectively) from ERS-1 (European Remote Sensing Satellite), JERS-1 (Japanese Earth Resources Satellite), and ALOS-PALSAR (Advanced Land Observing Satellite – Phased Array L-band SAR) data.

Currently the most objective and consistent systems for MRV are remote sensing-based, as ground-based monitoring systems are more susceptible to differing methodologies for carbon stock assessment, differing interpretations of key terminology, and unreliable reporting. For

this study, the UN Food and Agriculture Organisation (FAO) definition of forest is used: "Land spanning more than 0.5 hectares with trees higher than 5 meters and a canopy cover of more than 10 percent, or trees able to reach these thresholds in situ. It does not include land that is predominantly under agricultural or urban land use." (FAO, 2010). There are now several freely available remote sensing datasets that provide wall-to-wall coverage of Central African rainforests (Brady *et al.*, 2010), including medium resolution data from Landsat and ALOS-PALSAR. A list of major remote sensing mosaic projects from which forest cover maps were produced over Central Africa is seen below in Table 2.

Table 2: Major remote sensing mosaic projects with complete coverage of Central Africa.

Project name	**Sensor; sensor type**	**Spatial resolution**	**Year(s)**	**Project organisation; reference**
Central African Mapping Project	ERS-1; C-band SAR	100m	1994	Joint Research Centre (JRC); De Grandi *et al.* (1999)
Global Rainforest Mapping (GRFM) project	JERS-1; L-band SAR	100m	1996 (x2)	NASDA (now JAXA); Rosenqvist *et al*. (2000)
GLC2000	SPOT-VEGETATION; optical	1km	2000	JRC; Mayaux *et al.* (2004)
Vegetation Continuous Fields (VCF)	Terra-MODIS; optical	250m, 500m, 1km	2000-2010 (Annual)	University of Maryland (UMD), NASA; Hansen *et al.* (2003), DiMiceli *et al.* (2011)
Tree Cover Continuous Fields	Landsat; optical	30m	2000	UMD; Sexton *et al.* (2013)
Global Forest Change	Landsat; optical	30m	2000-2012	UMD, NASA, Google; Hansen *et al.* (2013)
GlobCover	ENVISAT-MERIS; optical	300m	2005/6, 2009	European Space Agency (ESA); Arino *et al*. (2007), ESA (2010)
ALOS Kyoto & Carbon Initiative	ALOS-PALSAR; L-band SAR	50m, 500m	2007-2010 (Annual)	JAXA, JRC; De Grandi *et al*. (2011)

2.2 AIMS AND OBJECTIVES

The overall aim of this study is to improve on existing forest area mapping techniques throughout the Congo basin and wider Central African tropical forests, using available data from several dates, and from this calculate changes in forest area. To this end, best possible methods for classifying available SAR data are explored, using available higher resolution optical remote sensing data for validation.

Using dual polarised L-band SAR mosaics, combined with medium and high resolution optical data, the two objectives of this study are to answer the following questions:

- What is the potential of available L-band SAR compared with optical data for forest area mapping throughout the Congo Basin region?
- To what extent can regional (below continental scale) classification techniques using L-band SAR data improve accuracy of forest area mapping when compared with forest area products produced with a globally consistent algorithm?

Section one of this report deals with the first objective by analysing a single-threshold decision tree classification of the entire Congo basin, which serves to pinpoint areas of discrepancy between optical and SAR-derived classifications. Establishing the strengths and limitations of the SAR data guides the classification approach used in the second section. The principal dataset used for section one was re-released by JAXA in January 2014, in an improved format that included two additional years of data (2007 and 2010), almost global coverage, and a forest/non-forest product. The second objective is addressed in section two of the report using a deeper analysis of this new data, quantitatively comparing accuracy with an optical remote sensing dataset and JAXA's forest/non-forest product, derived from the same data.

3 METHODOLOGY

3.1 STUDY AREA

The focus of this study, the Congo basin, contains the second largest tropical rainforest in the world, with a forested area of roughly 2 million km^2 (Bwangoy *et al.*, 2010). The Congo rainforest often refers to all of the forested areas of Central Africa, rather than specifically those contained within the drainage area of the Congo river (Justice *et al.*, 2001; Hansen *et al.*,

2008) and it either wholly or partially covers the following six countries: Cameroon, the Central African Republic, Equatorial Guinea, Gabon, the Democratic Republic of the Congo (DRC) and the Republic of the Congo. Of these, the DRC and the Republic of Congo are countries with active UN-REDD national programmes, and Cameroon, the Central African Republic, and Gabon are REDD partner countries.

The JAXA ALOS PALSAR imagery obtained for objective one of this study covers a rectangular area of Central Africa, bounded in the North-West by coordinates (Lat 008°00'N, Long. 008°00'E) and in the South East by coordinates (Lat. 010°00'S, Long. 038°00'E), seen in tiles A13-A16 and A19-A22 in Figure 1. The tiling constitutes the original format of data delivery for the K&C Initiative, and the tiles for this study were selected to completely cover the Congo Basin. This covers an area of around 6.7 million km^2, although a large section of this is in the ocean and therefore may be discounted. Apparent in Figure 1 is the fact that this study area is divided roughly equally on either side of the equator, leading potentially to seasonal differences throughout the dataset even at concurrent data acquisition.

For the second objective of this report, analysis was performed on a five degree by five degree square with an upper left coordinate of Lat. 005°00'N, Long. 015°00'E (Figure 2). The more recent release (January 2014) of K&C Initiative JAXA ALOS PALSAR data is organised into grids of five degree lat/long mosaiced squares subdivided into 25 one degree by one degree tiles. The selected area covers part of four countries: Cameroon, the Central African Republic, the Republic of Congo, and the Democratic Republic of Congo, and contains a wide range of landcover types, including: rainfed croplands, mosaic cropland/vegetation, broadleaved deciduous forest, shrubland, herbaceous vegetation (savannah), permanently and regularly flooded forest, urban areas and water bodies[1]. To facilitate processing and allow testing of several classification techniques, a smaller, more manageable site was chosen for this section of the report.

[1] Landcover classes taken from ESA's Globcover 2009 product, (ESA, 2010)

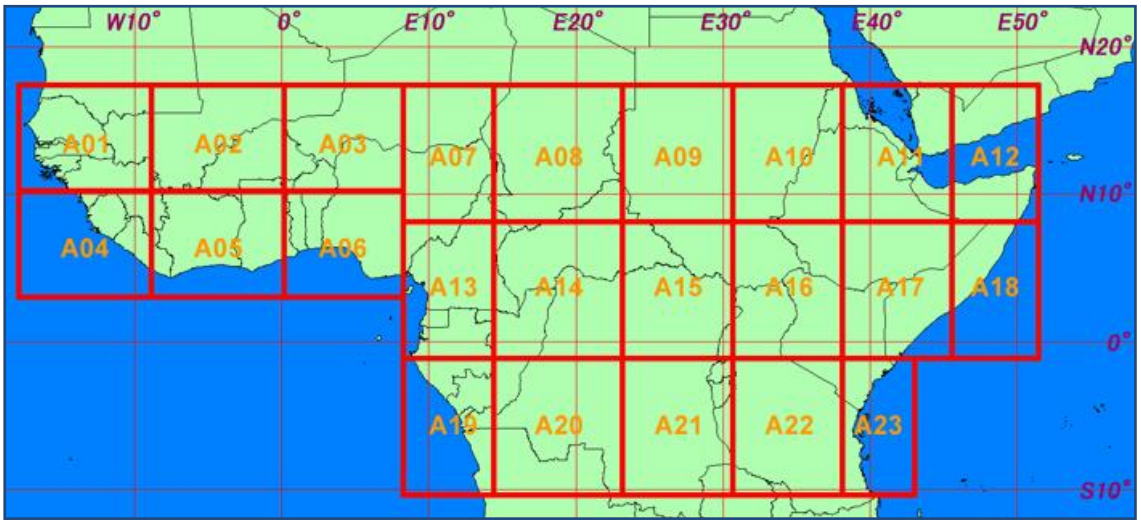

Figure 1: Original K&C initiative ALOS-PALSAR 50m mosaic availability over Central and West Africa. Image from JAXA (2010).

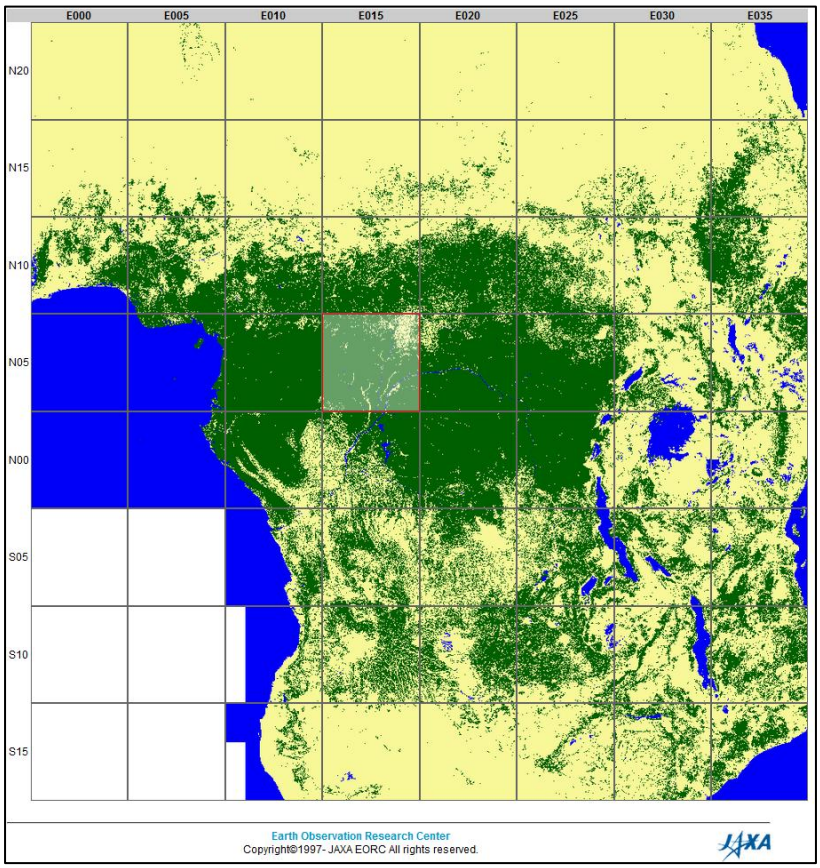

Figure 2: Current K&C Initiative ALOS-PALSAR availability over Central and West Africa, with highlighted study area for objective two. Underlying image is JAXA's Forest (dark green)/Non-forest (yellow) product (JAXA, 2014).

3.2 DATA

Until January 2014, there were two available 50m K&C Initiative ALOS-PALSAR mosaics, one from 2008 and the other from 2009, both derived from the backscatter intensity of the fine beam dual polarisation (HH and HV) acquisition mode. The 2009 mosaic was used to fulfil the aims of objective 1. They were generally acquired over a two-month period to reduce the effects of seasonal differences across the data strips, although in several cases bad data were replaced using data from adjacent years. The data were radiometrically calibrated to account for vegetation water content and soil moisture differences, using a strip balancing algorithm (De Grandi *et al.*, 2011). While this resulted in a relatively homogenous signal across the mosaics, there are several marked backscatter differences between adjacent data strips throughout the data, suggesting more extreme seasonal or local weather. Metadata from these earlier K&C PALSAR mosaics relating to the acquisition date and time of each individual data strip was not easily matched to available vector files showing the footprint of each acquisition, and there was also some drift in the location of the footprints between the 2008 and 2009 mosaics. Correspondence with the JAXA researchers responsible for producing the mosaic indicated that these issues would be resolved in later versions of the data, which they were.

Freely available Landsat data at 30m spatial resolution is available from the United States Geological Survey (USGS) covering the Congo basin. A recently (beta-) released 30m spatial resolution Landsat-derived dataset, Landsat Tree Cover Continuous Fields (LTC), is available with coverage for the year 2000 (Sexton *et al.*, 2013). This has been downloaded and mosaiced using MODIS vegetation continuous fields (VCF) data at a spatial resolution of ~250m to gap fill areas obscured by cloud cover (Figure 3). This data is currently the highest resolution freely available, replicable optical mosaic of such a wide area.

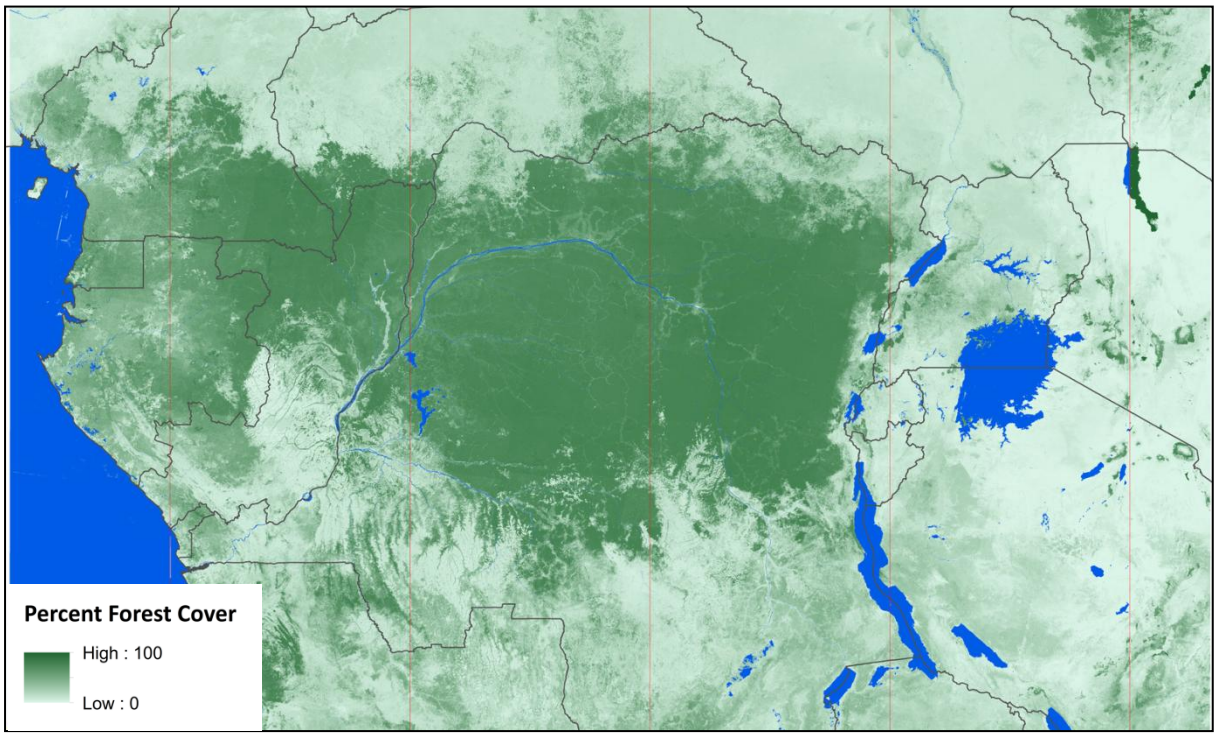

Figure 3: Mosaic of Landsat Tree Cover with MODIS VCF gap fill, covering the study area for objective 1.

For objective 2, the January 2014 release of the ALOS-PALSAR data was used, which contains similar dual polarisation mode information as before, although the data has been geocoded more consistently and accurately, allowing for easier comparison with other forest cover maps. The HH and HV channels are provided as normalised radar cross-section, gamma-nought, meaning the backscatter intensity has been adjusted for topography using the cosine of the local incidence angle as described in Shimada (2010). The data availability has been expanded to include the years 2007 and 2010, and the terrestrial coverage is now almost global. Metadata at a pixel level is provided in the form of local incidence angle, mask information, and days after launch of image acquisition (Figure 4). A global forest/non-forest product based on the ALOS-PALSAR data is provided, at the same scale. Striping in the data is minimal, although in each year in the area of interest of this study the mosaics all contain several data strips from preceding or proceeding years, used where data was missing or of poor quality from that particular year.

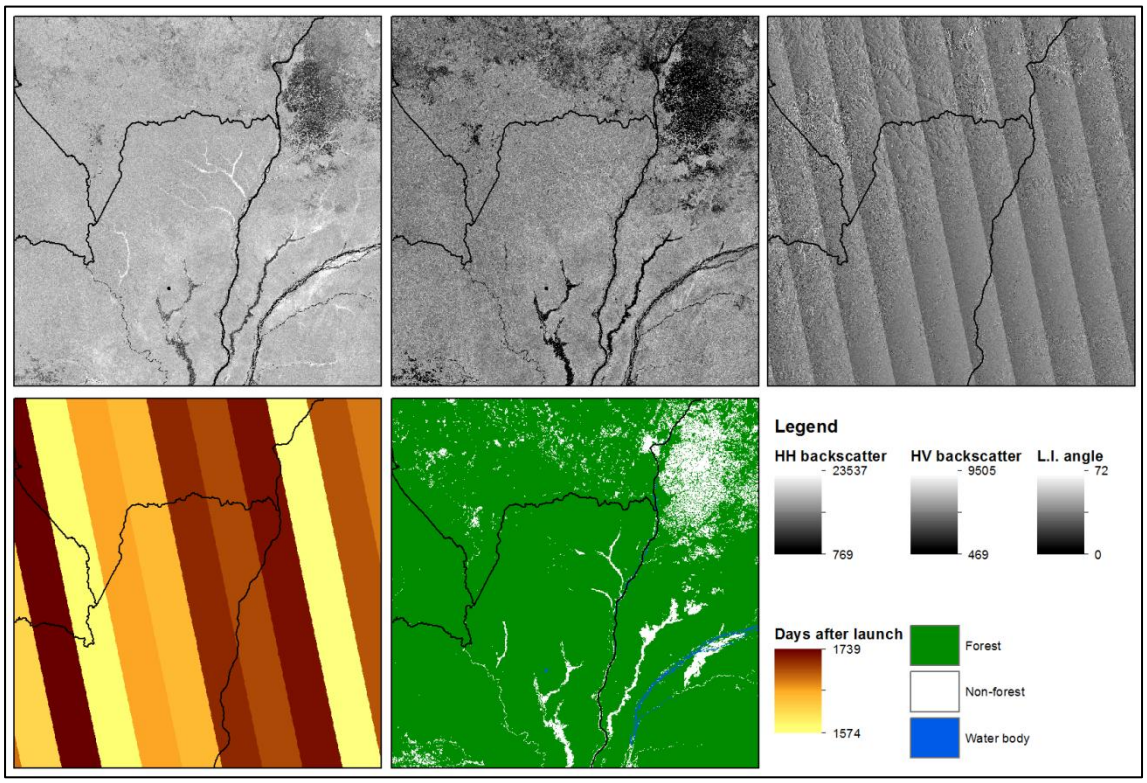

Figure 4: 2007 K&C Initiative products from JAXA in the study area for objective 2. Clockwise from top left: HH backscatter; HV backscatter; local incidence angle; forest/non-forest map; date of data strip acquisition (days after launch). Legend matches position of smaller windows.

Also released in early 2014 were the data from a global Landsat-derived product of forest loss/gain between 2000 and 2012 using Google's Earth Engine (Hansen *et al.*, 2013), including a more complete percentage tree canopy cover map than that produced by Sexton *et al*. (2013). So far, the tree canopy cover map is only available for 2000, but ancillary datasets, including forest gain/loss during the period 2000-2012 and a pixel level year of change map. The definition of forest from this product is described in terms of percentage of canopy cover of trees above 5m in height, and their threshold for loss/gain as described in Hansen *et al.*'s (2013) supplementary material is 50%, which is a high value, but one which may take into account the overestimation of forest cover from misclassification of cultivated cropland by optical sensors.

The training and validation dataset for objective two was derived from manual interpretation of optical Google Earth imagery. The steps for this process are described in more detail in section 3.4.

3.3 PROCESSING STEPS FOR OBJECTIVE 1: OPTICAL AND SAR FOREST COVER CLASSIFICATION COMPARISON

In order to coregister the PALSAR mosaics to, in particular, similar or higher resolution datasets such as Landsat, it needs to be precisely georeferenced, to at least one or two pixels. Without this precision, like is not being compared with like, especially in border areas of forest/non-forest. The 2008 and 2009 K&C Initiative PALSAR mosaics are poorly projected with a distortion that resulted in a varying offset of up to 10 pixels out of place with more reliable datasets, in this case the LTC. The problem is somewhat apparent in the Google Earth-projected data provided on the K&C Initiative website (http://www.eorc.jaxa.jp/ALOS/ge2/KC50/kc50top.kml), where the data is sometimes shifted by four or five pixels from the Google Earth imagery in the base map. This is obviously an unacceptable difference, as 10 pixels at 50m pixel resolution equates to a 500m shift of the ground target. In order to correct for this error, both mosaics, at both polarisations, were subset and reprojected to their corresponding Universal Trans Mercator (UTM) projections (Figure 5). This removed the distortion relative to the LTC data (also projected in UTM), and a manual correction to each subset's header files' tie points was sufficient to prepare them for coregistration.

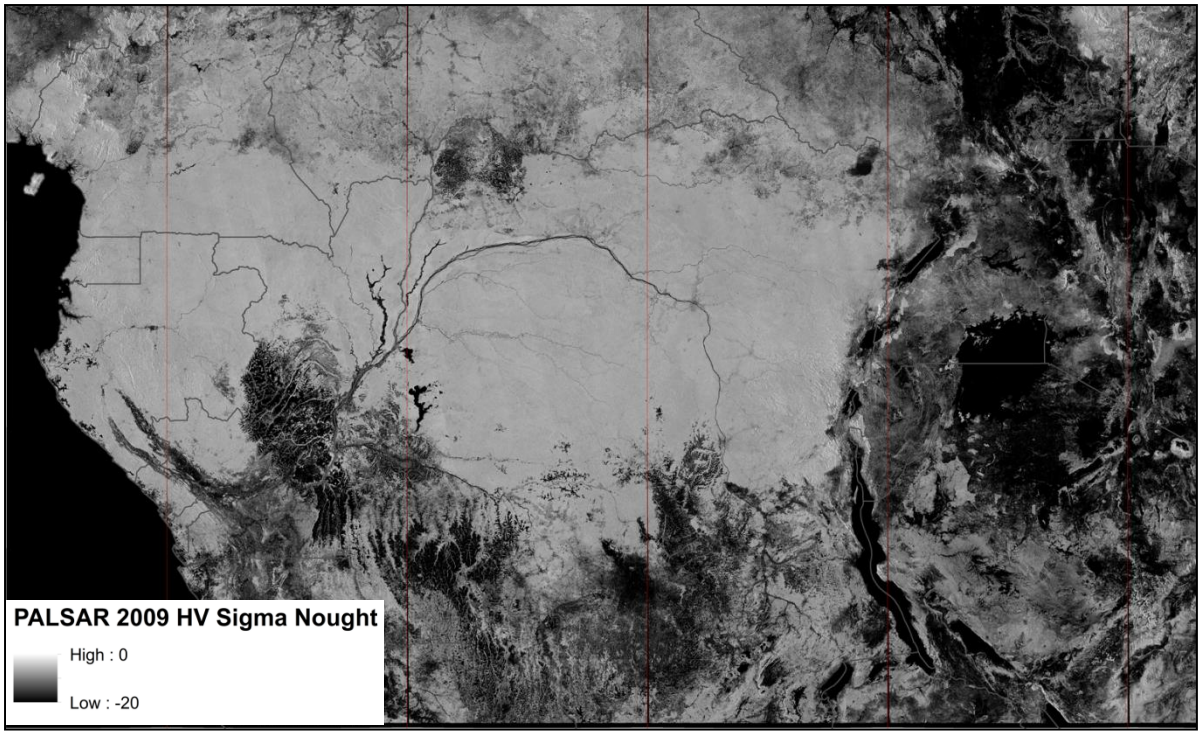

Figure 5: 2009 HV PALSAR mosaic subset and reprojected into UTM zones (vertical red lines).

For an initial, basic comparison between SAR-derived and optical-derived forest cover classification in the Congo basin, the 2009 HV polarised SAR data were selected. To begin with, each subset was converted to logarithmic sigma nought values from the raw intensity values using a calibration factor of -83 as described in the accompanying K&C Initiative metadata file. They were then coregistered to the LTC data at 30m spatial resolution and layerstacked according to UTM zone. A simple decision tree classification was then run according to Figure 6, using thresholds of 30% tree cover in the LTC data and -13.5dB in the SAR data. A second forest class, 'dense forest' was also calculated using a higher threshold (-12dB), but for the purposes of this study forest and dense forest are treated as one class. These threshold values were chosen through visual analysis of pixel values in forested areas in the case of the SAR data, and from the upper limit of tree cover as described by the UN Framework Convention on Climate Change (Decision 16/CMP.1, UNFCCC 2006) for the LTC data.

The results of the decision tree described in Figure 6 allow visual analysis of the potential of SAR with respect to an optical classification, by looking at disputed regions (coloured orange and light blue) and identifying which method has correctly classified the area as forest or non-forest.

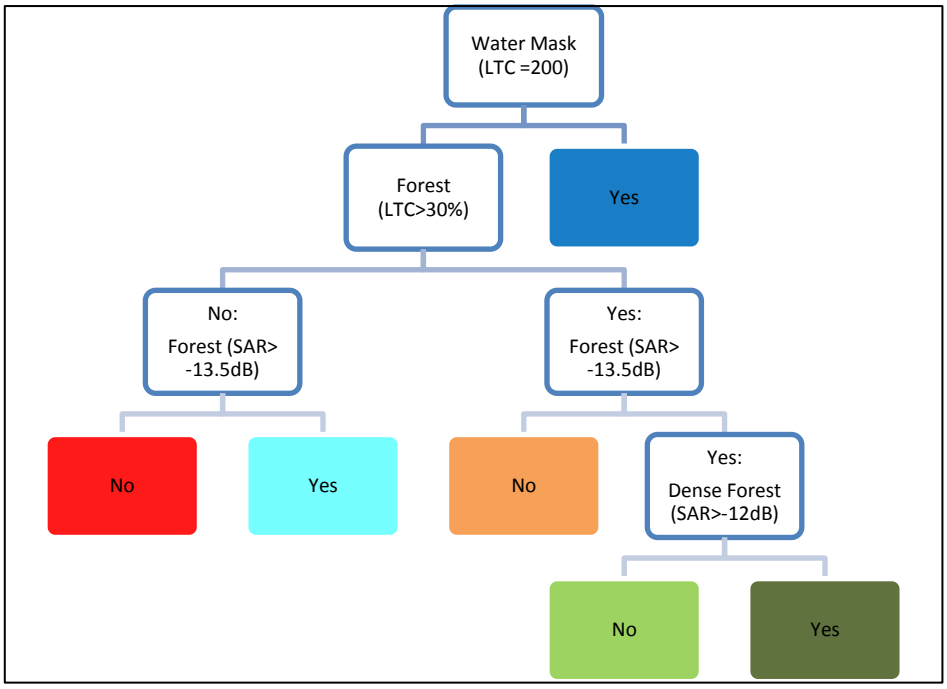

Figure 6: Decision Tree Classification of SAR (2009 PALSAR HV sigma nought values) and optical (LTC) data. Colours approximate classification legend from Figure 12.

3.4 PROCESSING STEPS FOR OBJECTIVE 2: SUPERVISED CLASSIFICATIONS OF IMPROVED K&C INITIATIVE ALOS-PALSAR MOSAICS

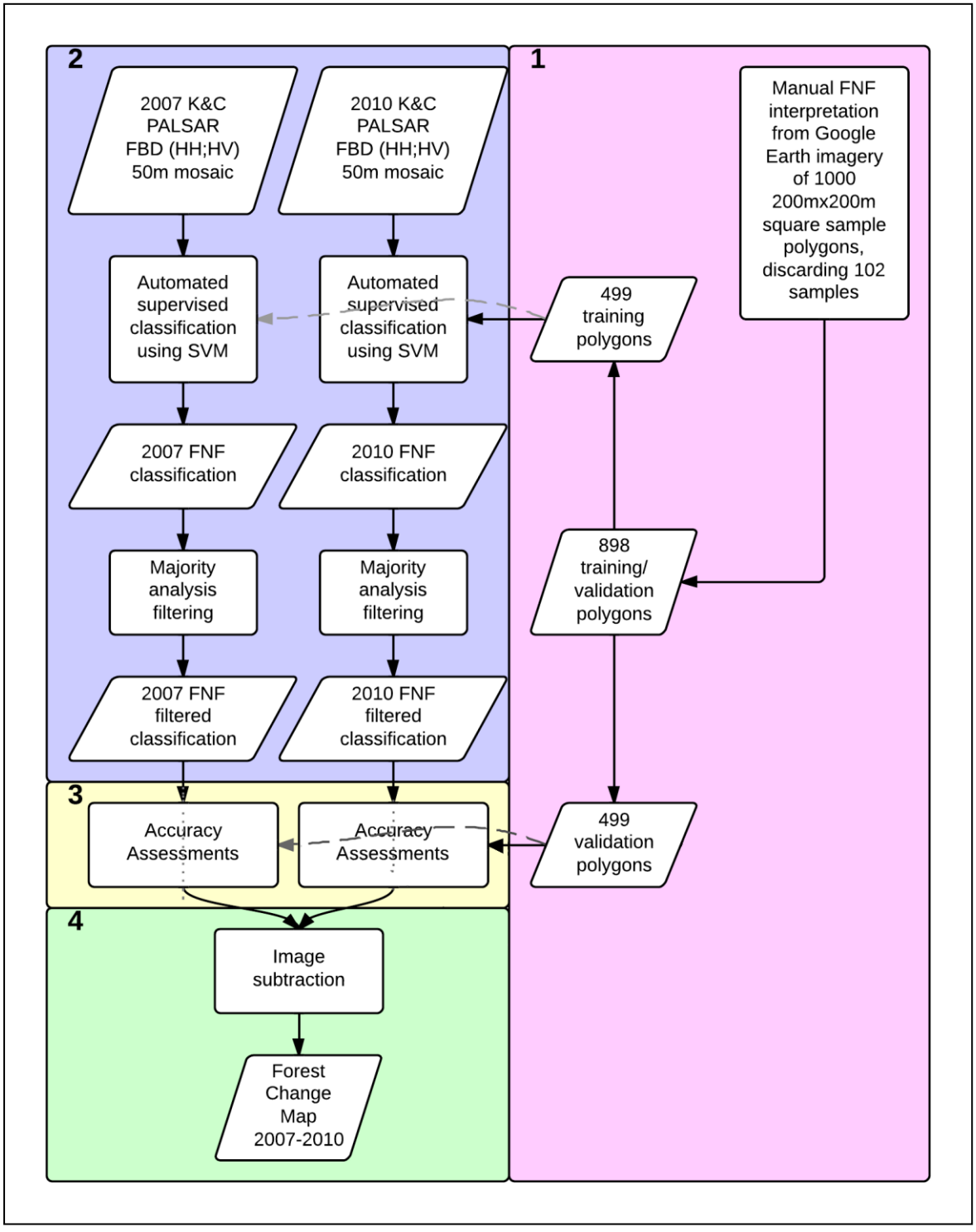

Figure 7: Processing steps for 2007-2010 forest change map based on support vector machine classification. Numbered coloured boxes show 1: selection of training/validation samples; 2: SVM classification steps; 3: accuracy assessment; 4: calculation of forest change.

As illustrated in box 1 of Figure 7, a training and validation dataset for objective two was created from a random sample of 1000 square (200m x 200m) plots covering the area of interest from Figure 2. Medium and high resolution Google Earth imagery (all acquired between 2012 and 2014, according to available metadata within the software) was used to determine the dominant forest/non-forest class in each sample square, and there was a loss of 102 samples due to mixing of classes, cloud cover, poor geocoding, and lack of clarity in the available training imagery. The resulting two sample sets (forest and non-forest) were each divided 50:50 into training and validation vector data.

All of the K&C Initiative data covering the study area for objective 2 from each year (2007-2010, inclusive) were mosaiced from 1 degree square tiles to 5 degree by 5 degree square tiles. These were compared with the Hansen *et al.* (2013) Landsat-derived datasets for projection and georeferencing consistency, and the error was found to be below one pixel. The HH and HV polarised channels were converted to sigma nought values using the same calibration factor of -83 as described in Section 3.3.

To more closely match the methodology of the JAXA forest/non-forest (FNF) product as described in Shimada *et al.* (2011) – resampled from 10m resolution to 50m resolution – two decision tree classifications were implemented using the sigma nought backscatter from the HV polarised PALSAR data, one with a high threshold of -14dB sigma nought backscatter, and one with a low threshold of -15dB, above which pixels were classified as forest. The JAXA map also describes an image segmentation approach, but this is not clearly described in their methodology and as such is difficult to replicate for the purposes of this study. However, a filtering algorithm using a majority analysis kernel was applied to the resulting class image to remove and reclassify spurious single pixels to the dominant surrounding class, effectively creating a minimum mapping unit of 3-4 pixels (~1ha).

A support vector machine (SVM) classification, using default ENVI parameters based on Chang & Lin (2011), was applied to the HH and HV sigma nought data for each individual data year. SVM is an advanced supervised classification algorithm that takes training data, typically from two classes, and classifies the image based on a decision surface referred to as an optimal

hyperplane, where the separability between classes is greatest. The same filtering algorithm as described above was applied to the resulting classifications to remove and reclassify spurious single pixels appropriately. This is shown in box 2 in Figure 7.

Following classification, an accuracy assessment was carried out using the validation samples from both classes (box 3 of Figure 7). This accuracy assessment was also applied to the JAXA FNF product, both decision tree (high and low) threshold methods described above, and finally to the Hansen *et al.* (2013) Landsat derived product (using a 30% tree canopy cover threshold to delineate forest/non-forest areas), firstly using all validation samples, and secondly using only those samples which fell in areas not stated to have changed (either through gain or loss) in the years 2000-2012. The forest change to 2012 rather than to 2010 (to match the K&C Initiative mosaic availability) period for the Hansen *et al.* (2013) product was used because the validation dataset is derived from up to date Google Earth imagery, so a more reliable estimate of accuracy may be obtained.

Forest area was calculated for each year with each method, and a loss/gain map was generated between 2007 and 2010 using a difference map from the SVM classifications for those years (box 4 in Figure 7).

4 RESULTS

4.1 OBJECTIVE 1: OPTICAL AND SAR FOREST COVER CLASSIFICATION COMPARISON

Figure 12 shows a resulting 2009 PALSAR HV mosaic-derived forest/non-forest classification comparison with Landsat Tree cover Continuous Fields (LTC) from 2000. Eight smaller windows illustrate and describe the limitations and strengths of both datasets. There are major discrepancies between the two approaches; in the north throughout most of the Central African Republic (CAR), in cropland areas, and in upland areas where there is a terrain effect on the SAR data. In this trial classification, disputed areas of forest/non-forest total 1,100,000 km^2, almost one fifth of the total land area processed (18.7%, not including water bodies). Of

this figure, 847,000 km^2 is classified as forest by the SAR dataset and non-forest (i.e. < 30% tree cover) by the LTC. The reasons for the differences are, in most cases, clear, and based on the physical properties of the sensors. In addition, the time difference between the SAR and optical datasets may be a factor in certain areas, where deforestation or reforestation has occurred in the intervening period.

4.2 OBJECTIVE 2: SUPERVISED CLASSIFICATION OF IMPROVED K&C INITIATIVE ALOS-PALSAR MOSAICS

Figure 8 shows the forest area by year calculated from the five classification methods examined. A general rise in forest area is observed using all methods, though a smoother change is seen using the SVM classifier. Annual fluctuations described by the basic thresholding classifiers (including the JAXA FNF method) appear unrealistic. This is illustrated by the comparison between JAXA FNF and the SVM approach in Figure 9. Regardless of their apparent improvement, cautious use of the SVM classifier results is advised in the absence of ground truth validation. A forest loss/gain map (Figure 10) between 2007 and 2010 shows a net increase in forest area of approximately 4,412 km^2, the equivalent of 1.4% of the study area.

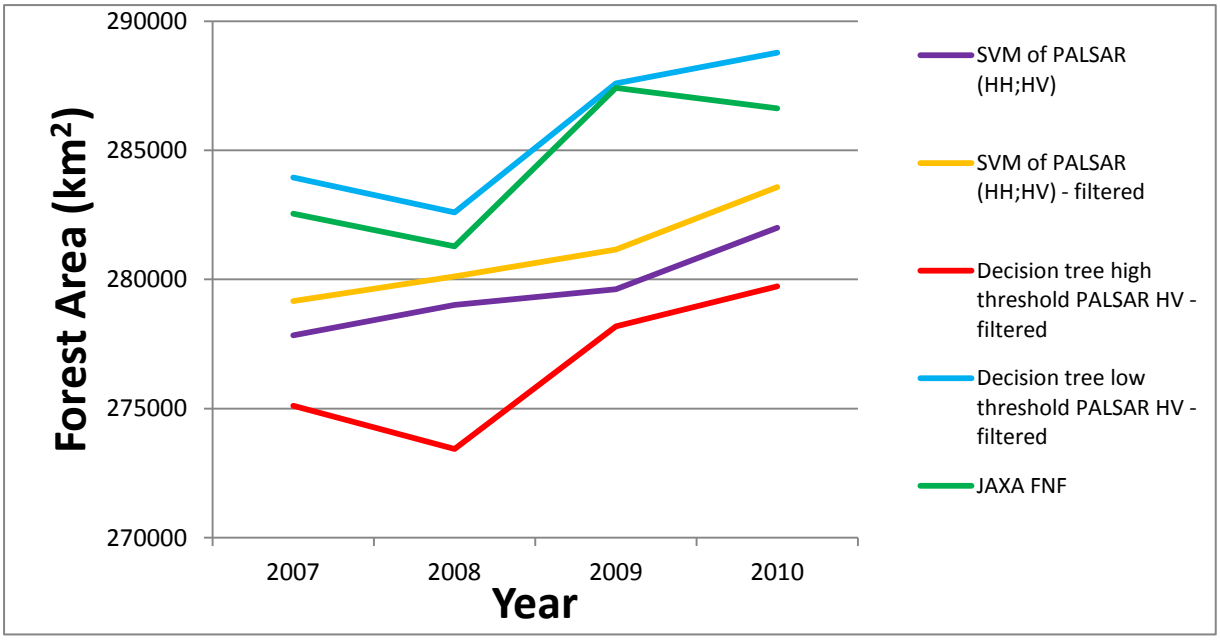

Figure 8: Graph of forest area by year showing differences in thresholding approaches.

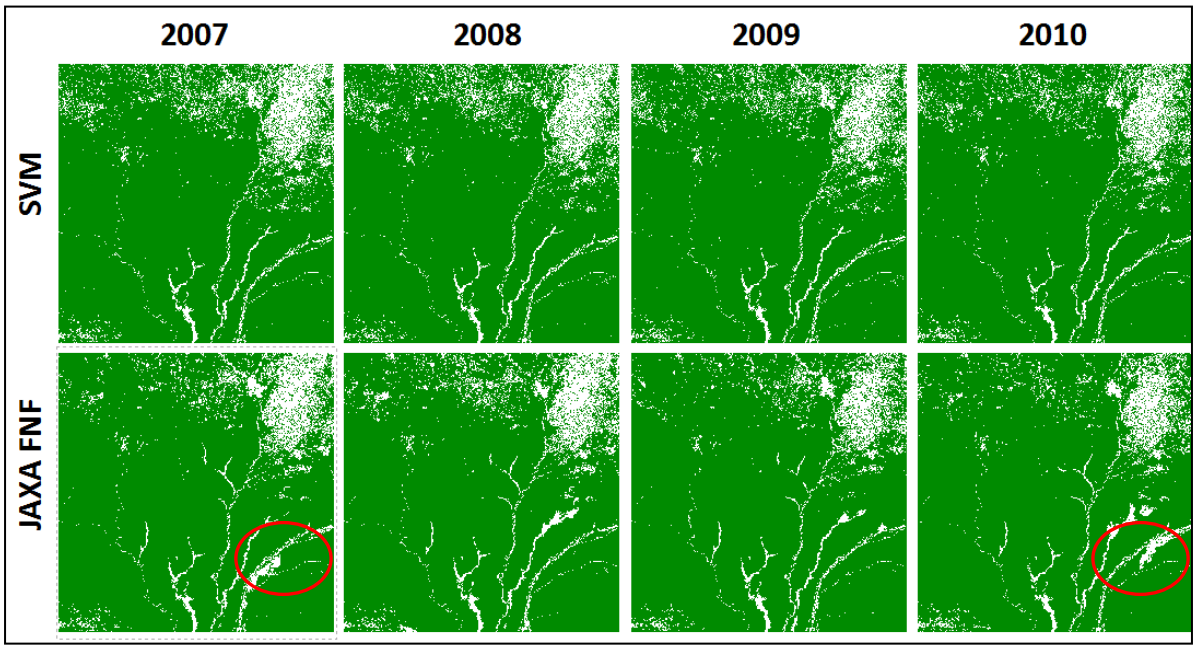

Figure 9: Side by side comparison of Forest/Non-Forest classifications from support vector machine (this study) and JAXA's FNF product. The red circle shows JAXA FNF classification problem in flooded forest.

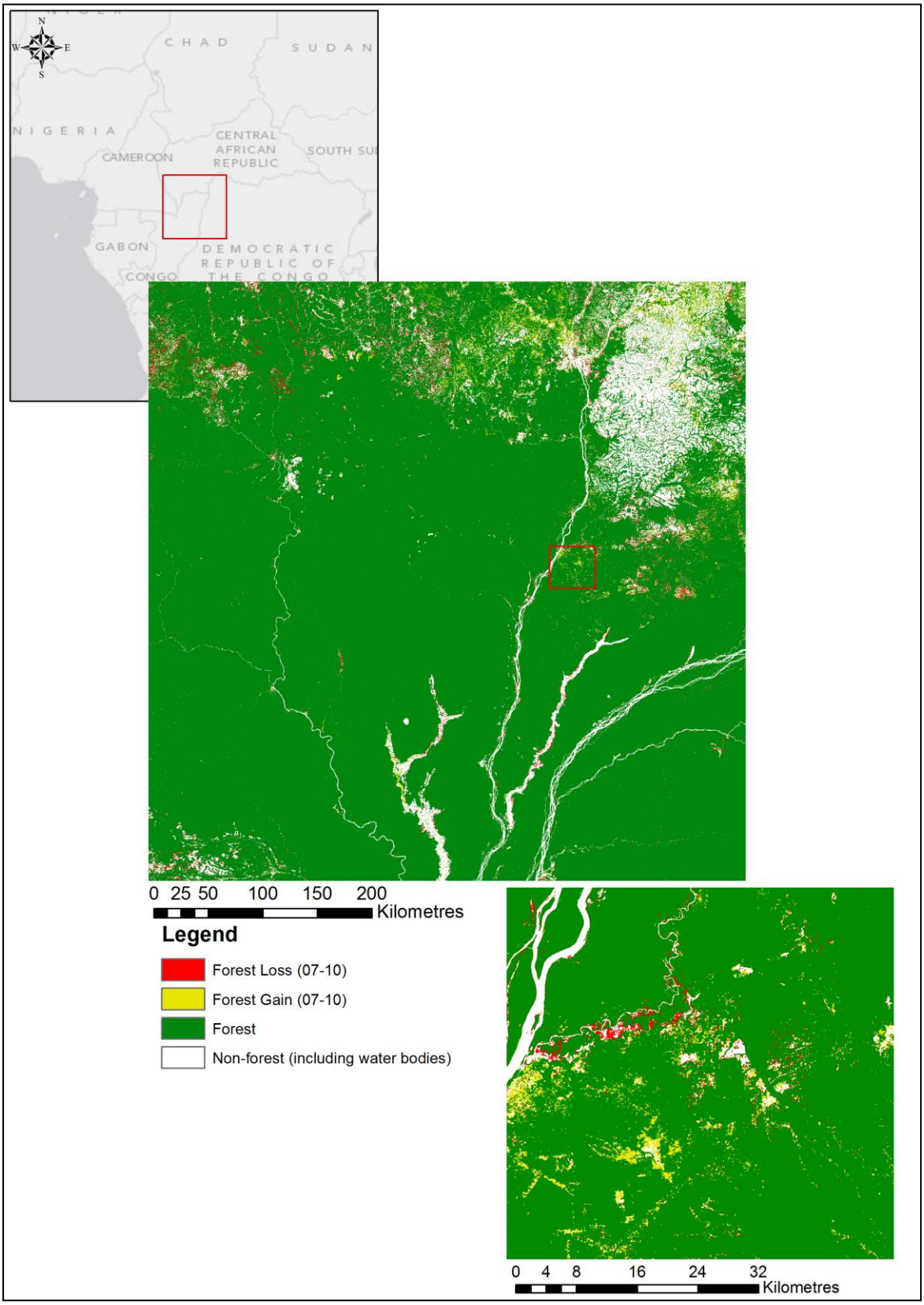

Figure 10: 2007-2010 map of forest gain/loss derived from SVM classification of HH and HV data.

Figure 11 shows the results of the accuracy assessments using the several classification methods described in section 3.4. Similarities between the low threshold (-15dB) decision tree classification and the JAXA FNF map suggest that this was closer to the threshold chosen by JAXA. High threshold (-14dB) decision tree classifications exhibited consistently higher accuracies than both the unfiltered and filtered SVM classifications, suggesting that sub-optimal parameters were used by the SVM classifier – specifically a low penalty parameter, described in the ENVI 5.0 documentation as allowing greater misclassification of training samples with the purpose of generating a more generalised classification where separability of classes is problematic, at the expense of accuracy.

Although the validation (and training) samples were generated by manual interpretation of recent (2012-2014) medium and high resolution imagery from Google Earth, a downward trend in accuracy was observed with time, from 2007 to 2010. The homogeneity selection criteria for the validation samples may account for this, as this tended to preclude forest/non-forest border zones, where difficulties in classification are more likely to occur.

These SAR derived classifications show a marked increase compared with the overall accuracy demonstrated by the Landsat-derived Hansen *et al.* (2013) forest cover map of the same area (90.9% and 64.6% using the full number of validation samples, and the subset number, respectively). This is when pixels stated to have changed between 2000 and 2012 have been accounted for, and using a 30% tree canopy cover threshold.

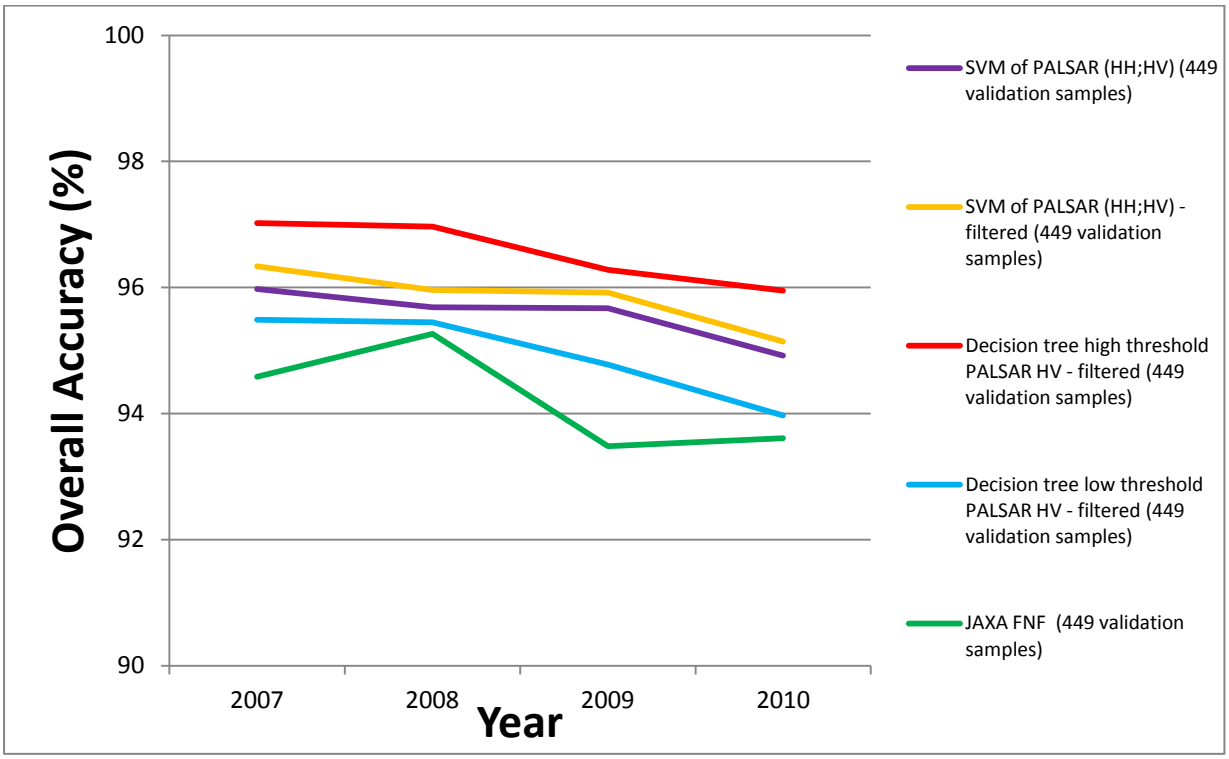

Figure 11: Graph of overall accuracy by year across all SAR derived classification methods used.

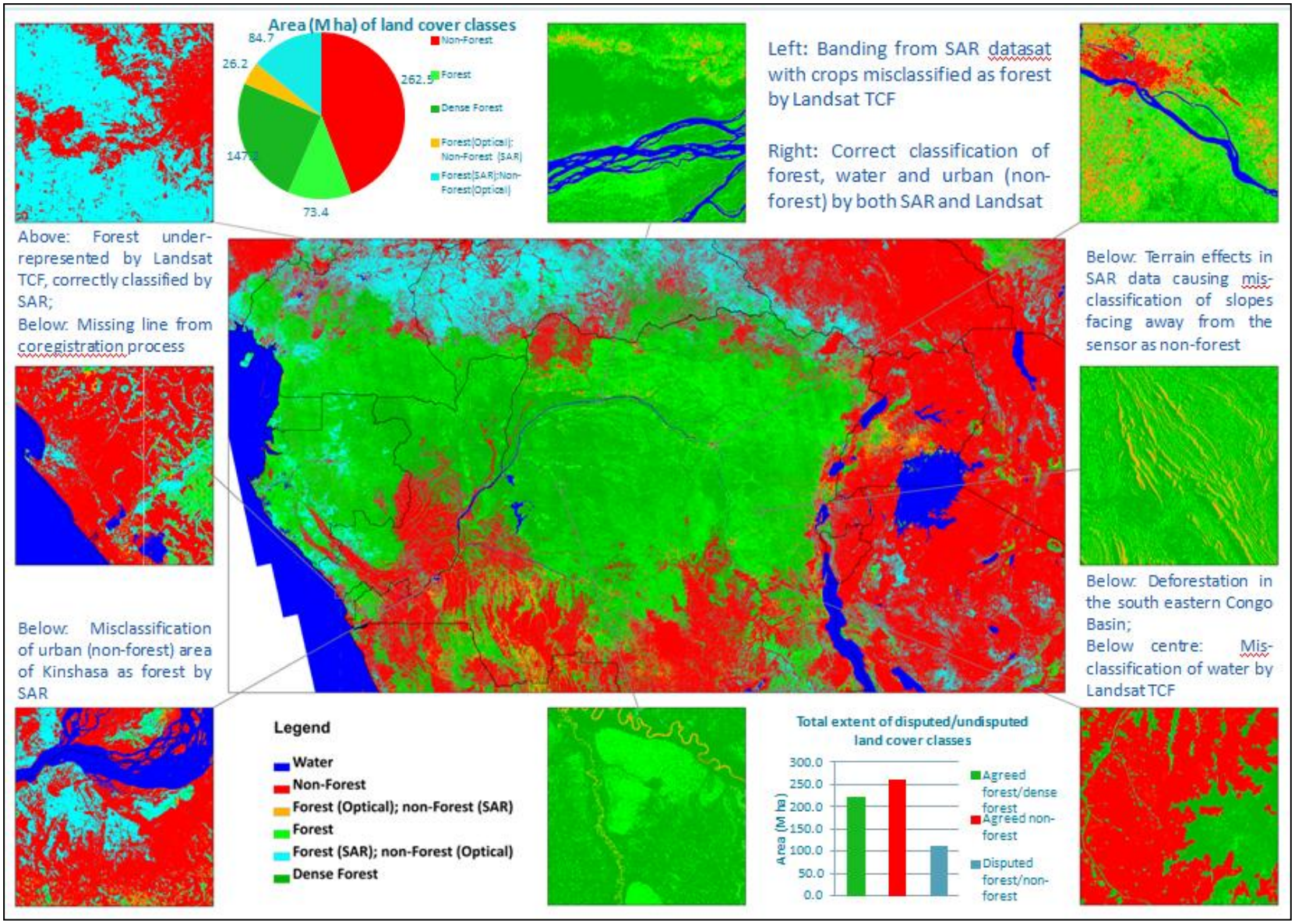

25

Figure 12: Forest/non-forest classification comparison of K&C SAR Mosaic with Landsat derived methods, with eight selected areas of interest and graphs showing extents of land cover classes, as well as aggregated disputed and undisputed land cover classes.

5 CONCLUSIONS

The questions posed for objectives 1 and 2 ("What is the potential of available L-band SAR compared with optical data for forest area mapping throughout the Congo Basin region?" and "To what extent can regional (below continental scale) classification techniques using L-band SAR data improve accuracy of forest area mapping when compared with forest area products produced with a globally consistent algorithm?") were answered by this study. For objective 1, the strengths and in some cases limitations of SAR with respect to optical data, as well as their areas of agreement, were illustrated by the eight areas of interest in Figure 12. These were calculated using relative differences in forest/non-forest classification from both datasets, and gave an indication of how a synergy of optical and SAR imagery might best be implemented. Principally, SAR and optical methods may complement each other in terms of correcting misclassification of urban and agricultural cropland areas as forest, respectively. Alternatively, a SAR-only classification could benefit from either a more thorough analysis of urban areas, or more simply with the use of an urban mask from ancillary datasets. The SAR terrain-related errors in classification were a cause for concern given the lack of sufficient metadata to resolve and correct for these issues, but the inclusion of local incidence angle information, as well as processed terrain correction, in the January 2014 release of the K&C data resolves this issue.

There is a clear improvement in accuracy and consistency of the classification methods used in Section 2 of this study over JAXA's FNF product. This may be attributed to their application of a global algorithm, compared with the supervised regional approach described in this study, but could also be indicative of a wider problem with applying a single polarisation channel threshold in forested areas that are prone to flooding. These results provide justification for applying this study's methodology across the whole Congo Basin.

A full comparison of the SVM SAR-based forest/non-forest map with (Hansen *et al.* 2013) will be possible when the methodology is applied to the entire Congo Basin. The increase in forest cover of 1.4% between 2007 and 2010 in the study area for objective 2 could be attributed to a variety of causes, including palm oil plantations being classified as forest by SAR.

5.1 FUTURE WORK

As described in section 4.2, the parameters of the SVM classifier may need to be tuned for an improved performance over the simple decision tree approach. A two-fold cross-validation approach, swapping training and validation samples is advisable to make the most use of all of the training and validation samples and provide enough data for robust statistical analyses of the results.

Applying an improved methodology of objective 2, here demonstrated as a proof of concept, to the entire Congo basin is the next step, and enables the generation of a complete and improved map of forest cover for the years 2007-2010. Following this, it will be possible to derive an estimation of forest change between the 1996 Global Rain Forest Mapping project L-band SAR derived product, described in (De Grandi *et al.*, 2000), as well as the 1994 Central Africa Mapping Project C-band SAR product, described in (De Grandi *et al.*, 1999), provided access to these datasets is obtained.

26 high resolution TerraSAR-X scenes from across the Congo Basin have been obtained and will be analysed and classified according to a novel (in the field of SAR remote sensing) texture measure, local binary pattern (LBP), described in (Ojala *et al.*, 2002), and the results compared with those using established (Haralick *et al.*, 1973) grey level co-occurrence matrix texture measures. These high resolution classifications may then be used as an additional training/validation dataset for the wide area study.

6 REFERENCES

Arino, O., Gross, D., Ranera, F., Bourg, L., Leroy, M., Bicheron, P., Latham, J., Di Gregorio, A., Brockman, C., Witt, R., Defourny, P., Vancutsem, C., Herold, M., Sambale, J., Achard, F., Durieux, L., Plummer, S. & Weber, J.-L. (2007) GlobCover: ESA service for Global Land Cover from MERIS. In: *IEEE International Geoscience and Remote Sensing Symposium (IGARSS) 2007*. pp.2412–2415.

Baccini, A., Laporte, N.T., Goetz, S.J., Sun, M. & Dong, H. (2008) A first map of tropical Africa's above-ground biomass derived from satellite imagery. *Environmental Research Letters*, 3 (4), p.045011.

Bala, G., Caldeira, K., Wickett, M., Phillips, T.J., Lobell, D.B., Delire, C. & Mirin, A. (2007) Combined climate and carbon-cycle effects of large-scale deforestation. *Proceedings of the National Academy of Sciences of the United States of America*, 104 (16), pp.6550–6555.

Brady, M., de Wasseige, C., Altstatt, A., Davies, D., Mayaux, P. & Tadoum, M. (2010) Executive Summary. In: M. Brady, C. de Wasseige, A. Altstatt, D. Davies, P. Mayaux, & M. Tadoum eds. *Monitoring Forest Carbon Stocks and Fluxes in the Congo Basin*. Brazzaville, Republic of Congo, p.iv.

Bwangoy, J.R.B., Hansen, M.C., Roy, D.P., De Grandi, G. & Justice, C.O. (2010) Wetland mapping in the Congo Basin using optical and radar remotely sensed data and derived topographical indices. *Remote Sensing of Environment*, 114 (1), pp.73–86.

CBD (2010) Strategic Plan for Biodiversity 2011-2020: Provisional Technical Rationale, possible indicators and suggested milestones for the Aichi Biodiversity Targets. In: *Conference of the Parties to the Convention on Biological Diversity*. Nagoya, Japan, pp.1–20.

Chang, C.-C. & Lin, C.-J. (2011) LIBSVM : A Library for Support Vector Machines. *ACM Transactions on Intelligent Systems and Technology*, 2:27:1--27, pp.1–39.

DiMiceli, C.M., Carroll, M.L., Sohlberg, R.A., Huang, C., Hansen, M.C. & Townshend, J.R.G. (2011) Annual Global Automated MODIS Vegetation Continuous Fields (MOD44B) at 250 m Spatial Resolution for Data Years Beginning Day 65, 2000 - 2010, Collection 5: Percent Tree Cover, University of Maryland, College Park, MD, USA. [Internet]. Available from: <http://glcf.umd.edu/data/vcf/>.

Englhart, S., Keuck, V. & Siegert, F. (2012) Modeling Aboveground Biomass in Tropical Forests Using Multi-Frequency SAR Data — A Comparison of Methods. *IEEE Journal of Selected Topics in Applied Earth Observations and Remote Sensing*, 5 (1), pp.298–306.

ESA (2010) Globcover 2009: products desciption and validation report [Internet]. Available from: <http://due.esrin.esa.int/globcover/LandCover2009/GLOBCOVER2009_Validation_Report_2.2.pdf>.

FAO (2010) Global Forest Resources Assessment 2010 [Internet]. Available from: <http://www.fao.org/docrep/013/i1757e/i1757e.pdf>.

De Grandi, G., Bouvet, A., Lucas, R.M., Shimada, M., Monaco, S. & Rosenqvist, A. (2011) The K&C PALSAR mosaic of the African continent: processing issues and first thematic results. *IEEE Transactions on Geoscience and Remote Sensing*, 49 (10), pp.3593–3610.

De Grandi, G., Malingreau, J.P. & Leysen, M. (1999) The ERS-1 Central Africa mosaic: A new perspective in radar remote sensing for the global monitoring of vegetation. *IEEE Transactions on Geoscience and Remote Sensing*, 37 (3), pp.1730–1746.

De Grandi, G., Mayaux, P., Rauste, Y., Rosenqvist, A., Simard, M. & Saatchi, S.S. (2000) The Global Rain Forest Mapping Project JERS-1 radar mosaic of tropical Africa: development and product characterization aspects. *IEEE Transactions on Geoscience and Remote Sensing*, 38 (5), pp.2218–2233.

Hansen, M.C., DeFries, R.S., Townshend, J.R.G., Carroll, M., Dimiceli, C. & Sohlberg, R.A. (2003) Global percent tree cover at a spatial resolution of 500 meters: First results of the MODIS vegetation continuous fields algorithm. *Earth Interactions*, 7 (10), pp.1–15.

Hansen, M.C., Potapov, P.V., Moore, R., Hancher, M., Turubanova, S.A., Tyukavina, A., Thau, D., Stehman, S.V., Goetz, S.J., Loveland, T.R., Kommareddy, A., Egorov, A., Chini, L., Justice, C.O. & Townshend, J.R.G. (2013) High-resolution global maps of 21st-century forest cover change. *Science*, 342, pp.850–853.

Hansen, M.C., Roy, D.P., Lindquist, E.J., Adusei, B., Justice, C.O. & Altstatt, A. (2008) A method for integrating MODIS and Landsat data for systematic monitoring of forest cover and change in the Congo Basin. *Remote Sensing of Environment*, 112 (5), pp.2495–2513.

Hansen, M.C., Stehman, S.V. & Potapov, P.V. (2010) Quantification of global gross forest cover loss. *Proceedings of the National Academy of Sciences of the United States of America*, 107 (19), pp.8650–5.

Haralick, R.M., Shanmugam, K. & Dinstein, I. (1973) Texture Features for Image Classification. *IEEE Transactions on Systems, Man and Cybernetics*, 3 (6), pp.610–621.

Herold, M. & Johns, T. (2007) Linking requirements with capabilities for deforestation monitoring in the context of the UNFCCC-REDD process. *Environmental Research Letters*, 2 (4), p.045025.

JAXA (2014) New Global Forest/Non-Forest Maps from ALOS PALSAR data (2007-2010) [Internet]. Available from: <http://www.eorc.jaxa.jp/ALOS/en/palsar_fnf/data/2007/html/Grid26_fnf.htm (requires registration)>.

JAXA (2010) PALSAR 50m Orthorectified Mosaic Product - Central Africa [Internet]. Available from: <http://www.eorc.jaxa.jp/ALOS/en/kc_mosaic/kc_50_c_africa.htm>.

Justice, C.O., Wilkie, D.S., Zhang, Q., Brunner, J. & Donoghue, C. (2001) Central African forests, carbon and climate change. *Climate Research*, 17, pp.229–246.

Malhi, Y. & Grace, J. (2000) Tropical forests and atmospheric carbon dioxide. *Trends in ecology and evolution*, 15 (8), pp.332–336.

Mayaux, P. & Achard, F. (2010) "REDD-plus" requirements for the Congo Basin countries. In: M. Brady & C. de Wasseige eds. *Monitoring Forest Carbon Stocks and Fluxes in the Congo Basin*. Brazzaville, Republic of Congo, pp.4–9.

Mayaux, P., Bartholomé, E., Fritz, S. & Belward, A. (2004) A new land-cover map of Africa for the year 2000. *Journal of Biogeography*, 31, pp.861–877.

NASA (2012) IceSAT-2 Home page [Internet]. Available from: <http://icesat.gsfc.nasa.gov/icesat2/> [Accessed 29 August 2012].

Ojala, T., Pietikainen, M. & Maenpaa, T. (2002) Multiresolution gray-scale and rotation invariant texture classification with local binary patterns. *IEEE Transactions on Pattern Analysis and Machine Intelligence*, 24 (7), pp.971–987.

Potapov, P.V., Turubanova, S.A., Hansen, M.C., Adusei, B., Broich, M., Altstatt, A., Mane, L. & Justice, C.O. (2012) Quantifying forest cover loss in Democratic Republic of the Congo, 2000–2010, with Landsat ETM+ data. *Remote Sensing of Environment*, 122, pp.106–116.

Rosenqvist, A., Finlayson, C.M., Lowry, J. & Taylor, D. (2007) The potential of long-wavelength satellite-borne radar to support implementation of the Ramsar Wetlands Convention. *Aquatic Conservation: Marine and Freshwater Ecosystems*, 17 (3), pp.229–244.

Rosenqvist, A., Shimada, M., Chapman, B., Freeman, A., De Grandi, G., Saatchi, S.S. & Rauste, Y. (2000) The global rain forest mapping project-a review. *International Journal of Remote Sensing*, 21 (6), pp.1375–1387.

Saatchi, S.S., Harris, N.L., Brown, S., Lefsky, M.A., Mitchard, E.T.A., Salas, W., Zutta, B.R., Buermann, W., Lewis, S.L., Hagen, S., Petrova, S., White, L., Silman, M. & Morel, A.C. (2011) Benchmark map of forest carbon stocks in tropical regions across three continents. *Proceedings of the National Academy of Sciences of the United States of America*, 108 (24), pp.9899–904.

Sexton, J.O., Song, X.-P., Feng, M., Noojipady, P., Anand, A., Huang, C., Kim, D.-H., Collins, K.M., Channan, S., DiMiceli, C. & Townshend, J.R.G. (2013) Global, 30-m resolution

continuous fields of tree cover: Landsat-based rescaling of MODIS Vegetation Continuous Fields with lidar-based estimates of error. *International Journal of Digital Earth*, 1303210312.

Shimada, M. (2010) Ortho-Rectification and Slope Correction of SAR Data Using DEM and Its Accuracy Evaluation. *IEEE Journal of Selected Topics in Applied Earth Observations and Remote Sensing*, 3 (4), pp.657–671.

Shimada, M., Isoguchi, O., Motooka, T., Shiraishi, T., Mukaida, A., Okumura, H., Otaki, T. & Itoh, T. (2011) Generation of 10m resolution PALSAR and JERS-SAR mosaic and forest/non-forest maps for forest carbon tracking. In: *IEEE International Geoscience and Remote Sensing Symposium (IGARSS) 2011*. Vancouver, BC, pp.3510–3513.

Stocker, T.F., Qin, D., Plattner, G.-K., Alexander, L.., Allen, S.K., Bindoff, N.L., Bréon, F.-M., Church, J.A., Cubasch, U., Emori, S., Forster, P., Friedlingstein, P., Gillett, N.P., Gregory, J.M., Hartmann, D.L., Jansen, E., Kirtman, B., Knutti, R., Krishna Kumar, K., Lemke, P., Marotzke, J., Masson-Delmotte, V., Meehl, G.A., Mokhov, I.I., Piao, S., Ramaswamy, V., Randall, D., Rhein, M., Rojas, M., Sabine, C., Shindell, D., Talley, L.D., Vaughan, D.G. & Xie, S.-P. (2013) Technical Summary. In: T. F. Stocker, D. Qin, G.-K. Plattner, M. Tignor, S. K. Allen, J. Boschung, A. Nauels, Y. Xia, V. Bex, & P. M. Midgley eds. *Climate Change 2013: The Physical Science Basis. Contribution of Working Group 1 to the Fifth Assessment Reoprt of the Intergovernmental Panel on Climate Change*. Cambridge, UK, Cambridge University Press, pp.33–115.

UNFCCC (2001) Report of the Conference of the Parties on its seventh session, held at Marrakesh from 29 October to 10 November 2001. Addendum. Part two: Action taken by the Conference of the Parties. Volume I [Internet]. Available from: <http://unfccc.int/resource/docs/cop7/13a01.pdf>.

UNFCCC (2010) Report of the Conference of the Parties on its sixteenth session, held in Cancun from 29 Novermber to 10 December 2010. Addendum. Part Two: Action taken by the Conference of the Parties at its sixteenth session. [Internet]. Available from: <http://unfccc.int/resource/docs/2010/cop16/eng/07a01.pdf>.

UNFCCC (2006) Report of the Conference of the Parties serving as the meeting of the Parties to the Kyoto Protocol on its first session, held at Montreal from 28 November to 10 December 2005 Addendum Part Two: Action taken by the Conference of the Parties serving as the [Internet]. Available from: <http://unfccc.int/resource/docs/2005/cmp1/eng/08a03.pdf>.

Verbeeck, H., Boeckx, P. & Steppe, K. (2011) Tropical forests: include Congo basin. *Nature*, 479, p.179.

White, L. (2012) The range and variety of African moist forests and their conservation [Internet]. Available from: <http://www.eci.ox.ac.uk/africa/downloads/session21.pdf> [Accessed 13 July 2012].